



Wind and Solar Resources Assessment Techniques for Wind-Solar Map Development in Jeddah, Saudi Arabia

Abobakr Al-Ttowi¹, Djamal Hissein Didane^{2,*}, Mohammad Kamil Abdullah², Bukhari Manshoor²

¹ Department of Energy and Thermofluid Engineering, Faculty of Mechanical and Manufacturing Engineering, Universiti Tun Hussein Onn Malaysia (UTHM) 86400 Parit Raja, Batu Pahat, Johor, Malaysia

² Center for Energy and Industrial Environment Studies, Faculty of Mechanical and Manufacturing Engineering, Universiti Tun Hussein Onn Malaysia (UTHM), Parit Raja, 86400 Batu Pahat, Johor, Malaysia

ARTICLE INFO

Article history:

Received 17 February 2022

Received in revised form 2 May 2022

Accepted 5 May 2022

Available online 6 June 2022

Keywords:

Renewable energy; wind energy; solar energy; resources assessments

ABSTRACT

Recent decades show a massive demand increment toward clean sources of energy as the world is experiencing industrial and technological revolutions. Among the various clean energy resources, wind and solar can be utilized effectively. This study aims to study wind and solar energy potentials in Jeddah, Saudi Arabia while identifying seasonal variations of wind and solar energies in the city. The essentiality of the study relies on the added benefits to the country where this research can help in finding other alternatives of energy other than fossil fuel. The Weibull distribution function and the Angstrom techniques were respectively used for the wind and solar resources assessments. The meteorological data involved are for ten years (2010-2019) including wind speed and direction, direct and diffused solar radiations. The results show that the prevailing wind direction at 10 m and 80 m altitudes were north and north-northwest, respectively. Meanwhile, the mean wind speed at 80 m altitude is found to be 4.36 m/s and 3.72 m/s at 10 m altitudes. The highest wind power and wind energy densities were at 80 m altitude with the value of 192.19 W/m² and 247.29 kWh/m², respectively. In terms of solar resources, the site has an average potentiality of global solar radiation of 23.13 MJm². The highest average possible sunshine duration occurred mostly in February, June, and November with respective values between 12.00 and 12.034 hours for most of the years. Lastly, the highest Angstrom's ratio occurred during June 2016 scoring 0.7942 while the lowest on the other hand was in December 2015, scoring 0.4253.

1. Introduction

Energy is the primary key to the development of a nation. Energy consumption is increasing rapidly as the world is experiencing an industrial and technological revolution. Even though energy is helping technological advances, it has its negative contribution that needs to be taken into account. Pollution and global warming are prominent examples of what fossil fuels can do to the planet. As the awareness of energy utilization rises, energy alternatives have been established [1]. Nevertheless, due to the increasing energy demand, it has become necessary to study the various

* Corresponding author.

E-mail address: djamal@uthm.edu.my

<https://doi.org/10.37934/arfmts.96.1.1124>

energy sources such as wind and solar [2-4]. Wind energy resources, for instance, varies depending on specified criteria such as elevation on the ground from the sea level and the surrounding where wind might not reach the turbine sufficiently. Wind energy has the potential to provide approximately about 10 million MW of energy, which is enough to replace the use of fossil fuels [5]. Such potentials could be harvested by utilizing appropriate designs of wind turbines [6-9]. Additionally, solar energy has the capability to provide energy for a variety of applications [10]. Solar energy (photovoltaics, solar thermal, solar power), on the other hand, provides significant environmental benefits in comparison to the conventional energy sources, thus contributing, to the sustainable development of human activities [11]. Solar energy technology has plenty of advantages such as reduction of the emissions of the greenhouse gases, reduction of the required transmission lines of the electricity grids; and improvement of the quality of water resources [12].

Saudi Arabia has a desert climate characterized by scorching heat during the day, sudden temperature drops at night, and little and irregular rainfall bringing higher chances of solar energy utilization. Nevertheless, due to the varying altitude and temperature fluctuations, wind and solar energy can be affected by different climatic conditions between coastal areas and inland areas [13]. In the next two decades, Saudi Arabia's total power generation capacity is expected to reach a total of 120 gigawatts. The country's rapid population growth and low electricity prices have led to the expansion of electrical services in the region [14]. Saudi Arabia was positioned seventh on the planet in 2012 in the rundown of 10 best places in clean energy overall [15]. Saudi rough fare limit would fall by around 3 million BPD to under 7 million BPD by 2028 except if homegrown energy request development is checked [16].

Due to the complexity of the data available for estimating the potentiality of wind energy, Bilir *et al.*, [17] suggested that a technique known as Weibull distribution should be used to provide a clear view of the available potentials. The statistical two-boundary distribution method is widely used in estimating the frequency and density of wind speed circulation [18,19]. On contrary, the Angstrom-Prescott technique is the most commonly solar assessment method due to its simplicity and validity [20]. A study conducted by Didane *et al.*, [21,22] and Hassane *et al.*, [23] in Jordan and Chad, revealed that wind energy has a promising potential to provide electricity in the two countries. They studied 13 meteorological stations in the country's three main zones. In another study carried out by Ramli *et al.*, [24] the power density and frequency distribution of wind speeds were also calculated using Weibull distribution. The results of the study revealed that Jeddah recorded medium wind speeds producing low power density. Such a low speed recorded resulted from the low height of the wind speed in which it was assessed at 10 m height.

On the contrary, Zell *et al.*, [25] aimed to investigate and assess solar resources in Saudi Arabia. The data were collected from 30 meteorological stations across the country during the 12 months from October 2013 to September 2014. The annual average daily Diffuse Horizontal Irradiance (GHI) varied widely across the country ranging from about 5700 Wh/m² to 6700 Wh/m² with steadily higher values inland and lower values along the coasts. The data collected showed that solar technologies could perform well in most locations. However, high temperatures may affect the performance of some types of solar panels.

Saudi Arabia, especially the western coastal region, has a large potential for wind and solar energy. A coastal city such as Yanbu which is about 200 km away from Jeddah city, was proven to have a sufficiently good potential for wind and solar energy to be utilized [26]. Ramli *et al.*, [24] performed a wind and solar hybrid system with battery storage. The results indicated that the western coast of Saudi Arabia has the potential to receive solar and wind energy. Saudi Arabia is bordered by seven countries and has three bodies of water. The Red Sea and the Gulf of Aqaba coastal border of almost 1,800 km extends to the southern part of Yemen and follows a mountain

ridge for approximately 320 km as shown in Figure 1. Jeddah generally is categorized as dry with a lack of precipitation rate most of the year. However, November considers the rainiest month. The Geographic coordinates of King Abdulaziz International Airport (KAIA) meteorological station are 039-11 East, 21-42 North, and 15 m for longitude, latitude, and elevation, respectively.



Fig. 1. Map of Saudi Arabia

2. Methodology and Theoretical and Mathematical Formulation

After the desired Meteorological Data are collected, they were statistically analysed where the average mean wind speed, temperature, and status of the sky will be obtained. The analysed data are used for further equations that aimed to assess wind and solar resources which eventually determine the amount available of power to be utilized.

2.1 Wind Resources

Before the calculation of the wind energy potential, various steps are needed to be taken into account. These include the calculation of the wind density and the amount of energy that the wind produces. Various assessment techniques are used to evaluate the wind potential of a site. The most commonly used assessment technique is the Weibull distribution. This distribution is a special case of the Pierson class III distribution and can represent the wind variations at a given site. Before the calculation of the wind power density, the pre-assessment steps are followed. This equation is shown below as Eq. (1) where Γ is the gamma function, ρ is air density 1.225 kg/m^3 at sea level with a mean temperature of $15 \text{ }^\circ\text{C}$ and 1 atmospheric pressure [18,21,22].

$$\frac{P}{A} = \int_0^\infty \frac{1}{2} \rho v^3 f(v) dv = \frac{1}{2} \rho c^3 \Gamma\left(\frac{k+3}{k}\right) \tag{1}$$

The wind is a kinetic energy source that is affected by the mass of air in Earth's atmosphere. The air density, which is the mass of air relative to the volume of air, influences wind power density. It can also be estimated by dividing the cross-sectional area of wind by the velocity of the wind. Wind power density can be estimated by using Eq. (2) where ρ is the density of air, A is the cross-sectional area where the wind comes through, and V is the velocity of the wind [18,21,22].

$$P = \frac{1}{2} \rho A V^3 \tag{2}$$

As wind speed varies, the carried amount of energy varies too, this means it is desired to estimate which wind speed has the maximum energy carried. Such requirement can be determined by using Eq. (3) below, where c and k are the Weibull scale parameter and Weibull shape parameter, respectively. C , K , and Γ can be calculated using Eq. (4), Eq. (5), and Eq. (6) while Eq. (7) is specialized in estimating the energy density of the wind [18,21,22].

$$V_{\max.E} = C\left(1 + \frac{2}{k}\right)^{1/k} \quad (3)$$

$$V_{mp} = c \sqrt[k]{\left(\frac{k-1}{k}\right)} \quad (4)$$

$$K = 0.83V_{Avg}^{0.5} \quad (5)$$

$$C = \frac{V_{Avg}}{\Gamma(1+1/k)} \quad (6)$$

$$\frac{E}{A} = \frac{\rho c^3}{2} \frac{3}{k} \Gamma\left(\frac{3}{k}\right) T \quad (7)$$

2.2 Solar Resources

The Sun experiences diffuse and incident solar radiation due to the various factors that contribute to its attenuation. These include water vapor and dust particles. The solar flux at the earth's surface is given as the sum of incident and diffuse radiation. Global solar radiation H_h maybe represented by Eq. (8). K_T is the Clearness Index and H_o is the extraterrestrial solar radiation on a horizontal surface. H_o is only a function of latitude and is independent of other location-specific parameters. The daily clearness index K_T is also given as H_h/H_o . Due to the attenuation, H_h is highly dependent on the location of the place on the earth's surface; and its value is less than extra-terrestrial irradiation, H_o [23].

$$H_h = K_T H_o \quad (8)$$

This step is the finalizing one in assessing solar resources where the Angstrom equation is to be used as shown in Eq. (9); where it is the ratio of monthly averaged daily global to monthly averaged daily extra-terrestrial radiation on a horizontal surface. This ratio, known as the clearness index, gives the percentage deflection by the sky of the incoming global radiation and therefore indicates both the level of availability of solar radiation and changes in atmospheric conditions in each locality while relative sunshine duration, n/N is a measure of the cloud cover. Here, a and b are regression coefficients. The extraterrestrial solar radiation on a horizontal surface is calculated from the following Eq. (10), where d is the day of the year, I_{SC} is the solar constant with a value of 1367 Wm^2 , ϕ is the latitude of the location, δ is the declination angle, and ω is the sunset hour angle. The declination angle, sunset hour angle and maximum possible sunshine duration are presented in the following Eq. (11), Eq. (12), and Eq. (13), respectively [23].

$$\frac{H_h}{H_o} = a + b \frac{n}{N} \quad (9)$$

$$H_o = \frac{24 \times 3.6 \times 10^{-3} \times I_{sc}}{\pi} \times \left(1 + 0.033 \cos \left(360 \frac{d}{365} \right) \right) \cos \phi \cos \delta \sin \omega + \omega \sin \phi \sin \delta \quad (10)$$

$$\delta = 23.45 \sin \left(360 \frac{248+d}{365} \right) \quad (11)$$

$$\omega = \cos^{-1}(-\tan \phi \tan \delta) \quad (12)$$

$$N = S_0 = \left(\frac{2}{15} \right) (\omega)_{deg} \quad (13)$$

3. Results and Discussion

This section explains in detail the assessments of wind resources for different levels of altitudes as 10 m and 80 m, as well as solar resources for the city of Jeddah in Saudi Arabia. Moreover, it demonstrates seasonal variations for the period between 2010 to 2019. On the other hand, this section elucidates the prevailing wind directions demonstrated in the wind rose. The relationship between the climate parameters and the potentiality of utilizing wind and solar energies are discussed.

3.1 Monthly Wind Speed Variation

Understanding the wind speed variation is very important when it comes to choosing a wind turbine site. Figure 2 shows the wind speed variation for a decade from 2010 to 2019. Generally, it can be seen that the relationship between altitude and wind speed is proportional. June always scores the highest wind speed at 4.36 m/s and 3.73 m/s for 10 m and 80 m altitudes, respectively. Nevertheless, seasonal variations were major contributors to wind speed. This is clearly shown in October which achieve the lowest wind speed for the total assessed period.

Moreover, the highest wind speed over the years at 10 m altitude was in 2019 in the month of March with a score of 4.25 m/s, while the lowest was in 2012 in October as shown in Figure 3. In terms of seasonal variation, the highest wind speed falls always during the summer solstice which starts from June the 7th to September the 5th. During this season, the precipitation rate is at its lowest whereby it always approaches the zero mm. This shows an inverse relationship between the precipitation rate and wind speed; meaning the less the precipitation rates the higher the average wind speed.

For a better comparison between the years, the average monthly wind speed was obtained for each year which resulted in Figure 3. The figure illustrates the monthly variation of wind speeds for the period of ten years (2010-2019). It can be noticed that the highest average wind speed occurred in January 2011, while the lowest was in October 2012. Nevertheless, the average wind speed at 80 m altitude is higher than 10 m with an average of 80%. Such a higher average wind speed will surely result in a higher power density.

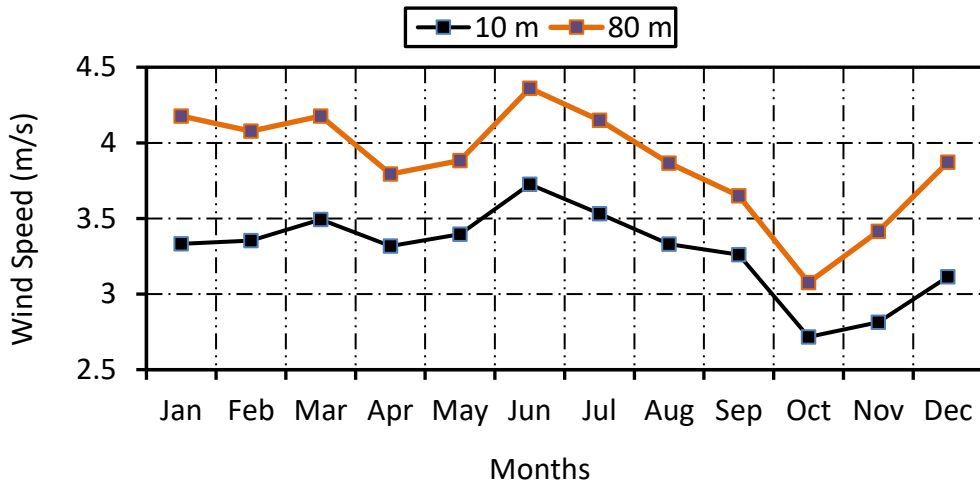


Fig. 2. Monthly average wind speed variation for 10 m and 80 m altitudes

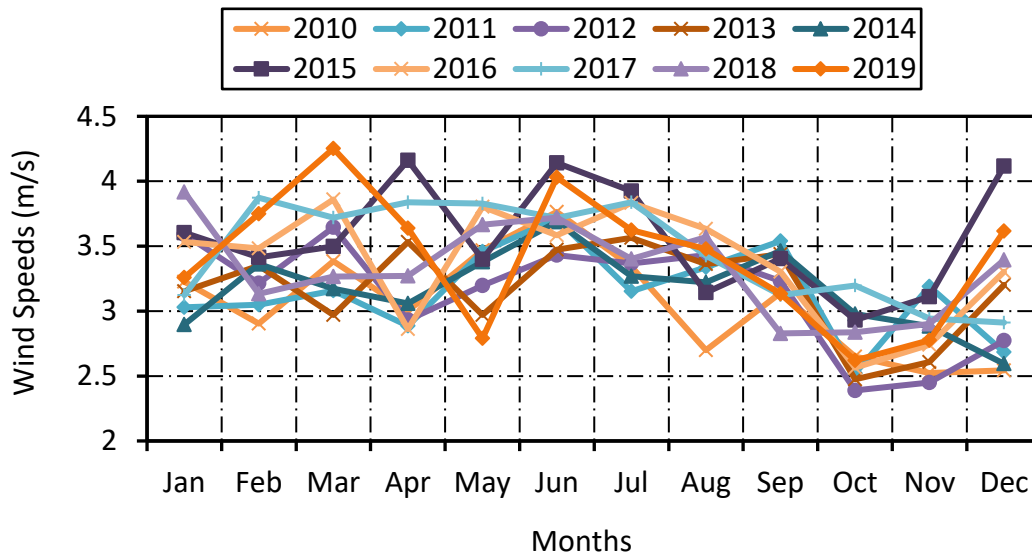


Fig. 3. Monthly wind speed variation for 10 m altitude for the period (2010-2019)

3.2 Wind Resources Parameters

In assessing wind resources, wind speed only is not sufficient. Hence, parameters such as wind speed carrying maximum energy, wind power density, and wind energy density are required. In detail, the Weibull probability distribution is used to determine the stated parameters. Wind power density and wind energy density for 10 m altitudes were found to be 44.09 W/m^2 and 285.46 kWh/m^2 respectively as shown in Table 1. In comparison between 10 m and 80 m altitudes, the wind parameters are appeared to be higher. Wind power density and wind energy density for 80 m altitudes were found to be 192.19 W/m^2 and 247.29 kWh/m^2 , respectively. This proves a proportional relationship between altitude and wind speed. However, even though wind parameters were affected positively by the altitude, the case was different for the wind energy density. This is due to the higher scale parameter 'k' mainly and the other parameters on the other hand.

Table 1
 Average wind parameters for 10 m and 80 m altitudes

Parameters								
KAIA Station	K	C	V_{mean}	$V_{Max,E}$	V_{mp}	Γ	P/A	E/A
	Unitless	m/s	m/s	m/s	m/s	Unitless	W/m ²	kWh/m ²
10 m altitude	1.75	3.56	3.28	5.50	2.20	0.59	44.09	285.46
80 m altitude	4.09	8.19	3.89	8.31	7.48	0.42	192.19	247.29

The mean power density for 10 m and 80 m altitudes shown in Figure 4 illustrates proves that higher levels of altitudes result in more power density. From the figure, it can be noticed that the highest average wind speed produces the highest mean wind power density which occurred in 2015. The highest wind power density for 10 m and 80 m altitudes were 58.33 W/m² and 362.29 W/m² respectively. Furthermore, even though the wind speed and wind power density are related, it is not a sufficient parameter to assess the wind. Moreover, the lowest mean power density in 2016 did not occur during the lowest average wind speed in 2010. Such a confusing relation is a result of the effect of other parameters such as 'c', 'k', and 'Γ' as scale parameter, shape parameter, and gamma function, respectively. Detailly, the values of scale and shape parameters in 2016 where the lowest average wind speed was achieved were less compared to the remaining years. Such a comparison is detailed in Table 2.

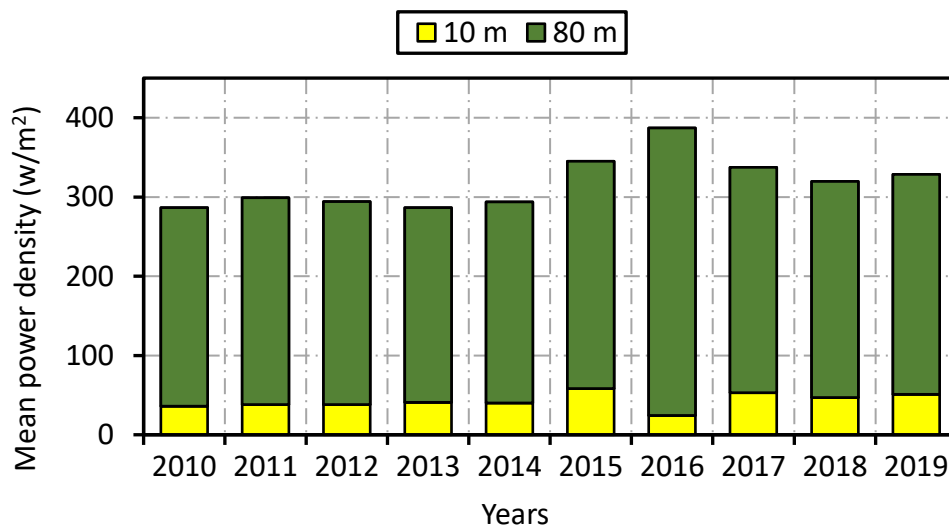


Fig. 4. Wind power density for 10 m and 80 m altitudes

Table 2
 Average yearly wind parameters for 10 m and 80 m altitudes

Year	Unit	2010	2011	2012	2013	2014	2015	2016	2017	2018	2019
10 m altitude											
V_{Avg}	m/s	3.05	3.14	3.14	3.17	3.16	3.57	3.37	3.46	3.325	3.41
$V_{Max,E}$	m/s	5.46	5.32	5.35	5.66	5.70	6.15	5.11	5.81	5.69	5.80
V_{mp}	m/s	1.79	2.00	2.00	1.91	1.849	2.35	0.84	2.40	2.22	2.34
Γ	Unitless	0.57	0.59	0.58	0.57	0.57	0.57	0.76	0.58	0.57	0.58
C	m/s	3.30	3.37	3.38	3.45	3.42	3.92	2.52	3.81	3.65	3.77
K	Unitless	1.61	1.70	1.70	1.62	1.60	1.72	1.31	1.78	1.733	1.76
P/A	W/m ²	36.10	38.04	38.27	40.77	40.30	58.33	24.57	52.89	47.09	51.18
E/A	kWh/m ²	263.48	257.18	258.92	294.21	296.62	389.13	234.41	335.09	309.97	329.82
80 m altitude											
V_{Avg}	m/s	3.78	4.00	3.78	3.54	3.60	4.17	3.96	4.10	3.92	4.14
$V_{Max,E}$	m/s	8.18	8.22	8.19	8.14	8.23	8.54	8.42	8.40	8.40	8.44
V_{mp}	m/s	7.4	7.46	7.58	7.36	7.26	7.63	7.65	7.53	7.46	7.41
Γ	Unitless	0.57	0.59	0.58	0.57	0.57	0.58	0.76	0.58	0.57	0.58
C	m/s	7.70	7.75	7.81	7.66	7.64	7.00	7.94	7.00	7.82	7.82
K	Unitless	5.32	5.34	6.00	5.30	4.73	5.00	5.40	4.84	4.88	4.63
P/A	W/m ²	250.32	261.03	255.70	245.89	253.42	286.91	362.28	284.49	272.56	277.47
E/A	kWh/m ²	304.87	313.14	255.34	302.52	374.08	386.92	430.84	403.83	382.69	423.75

3.3 Weibull Distribution

For clearer observation between the actual and predicted readings; Figure 5 and Figure 6 elucidate the highest and lowest wind frequency with respect to wind speed bins. For the 10 m altitude, the highest frequent Weibull wind speed is between 1.00 and 1.99 (m/s) scoring 22.14% which is lower compared with 26.66% for the measured wind speeds. The lowest frequency of wind speeds for measured and Weibull is between 13.00 to 13.99 (m/s) with 3 times of frequency. Even though bins 13 and 14 are the highest wind speed, they are not probable. This means for a wind turbine to be efficient, the wind speed should not be only high, but continuous and probably frequent as well. Moreover, for 80 m altitude, the highest frequency of wind speed was in the range between 4.00 to 4.99 (m/s) scoring 25.7%. By following a sequence of calculations as shown in the mathematical formulation section, Weibull parameters were obtained. Furthermore, the values with zero frequency were neglected which justifies the reason where the graph began from bin 4 (m/s).

The cumulative distribution for the KAIA station for 10 m and 80 m altitudes can be seen in Figure 7 and Figure 8. In comparison between the two altitudes, it can be noticed that the nature of trends varies. It is justified that 80 m altitude has higher speed records with more frequency occurrences compared with 10 m altitude.

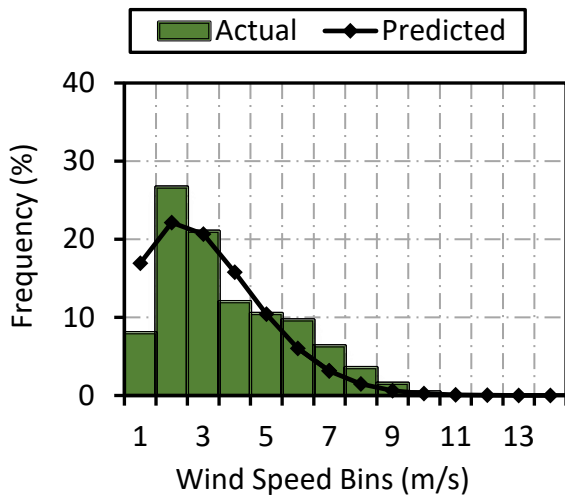


Fig. 5. These two figures have been placed side-by-side to save space

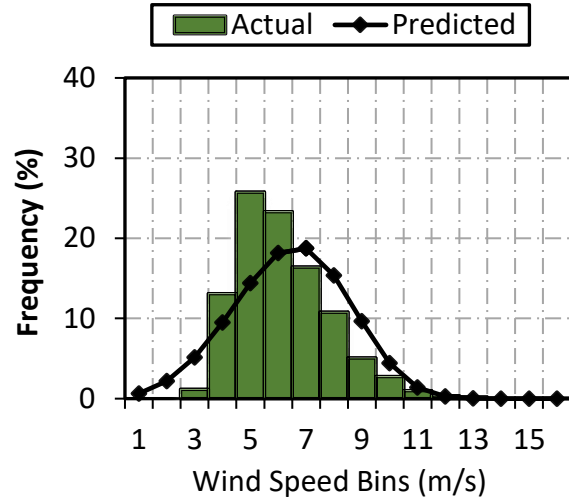


Fig. 6. These two figures have been placed side-by-side to save space

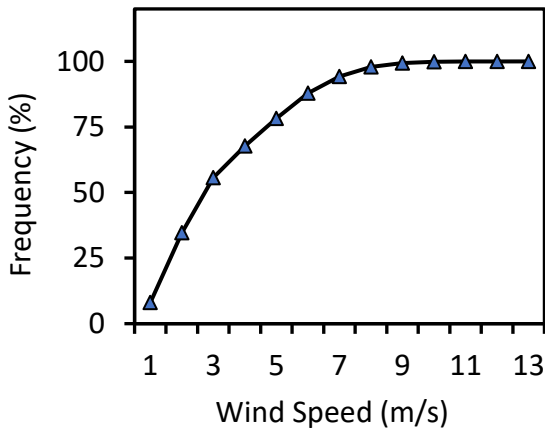


Fig. 7. Cumulative frequency of wind speed for 10 m altitude

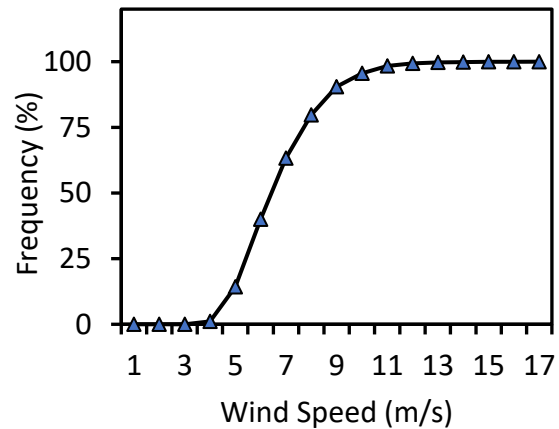


Fig. 8. Cumulative frequency of wind speed for 80 m altitude

3.4 Wind Direction

The importance of evaluating wind direction is associated with revealing the impact of geographical features on the wind and assessing wind speed and its direction flows with respect to the number of occurrences among a specified range. However, Figure 9 and Figure 10 illustrate the wind rose which explains the wind speed flows and its polar direction for both assessed altitudes 10 m and 80 m. For 10 m altitude, the highest number of occurrences is 11,864 times, flowing from the north direction achieving a wind speed between the range of 0 to 5 (m/s). In the second place is north-northwest with 9,453 times of occurrences achieving a wind speed in between the range 0 to 5 (m/s). Even though the range 10 to 15 (m/s) has higher values of wind speed, it is not probably occurred. The highest number of occurrences for such a range is 44 times, flowing from south-southeast.

For 80 m altitude, the highest number of occurrences is 11,572 times, flowing from the north-northwest direction achieving a wind speed between the range of 0 to 5 (m/s). In the second place in the north direction with 8,948 times of occurrences achieving a wind speed in between the range 0 to 5 (m/s). Different from the 10 m altitude, there were some occurrences in between the range

15 to 20 (m/s). Even though the range is higher in wind speed, it must be high in occurrences as well to be considered.

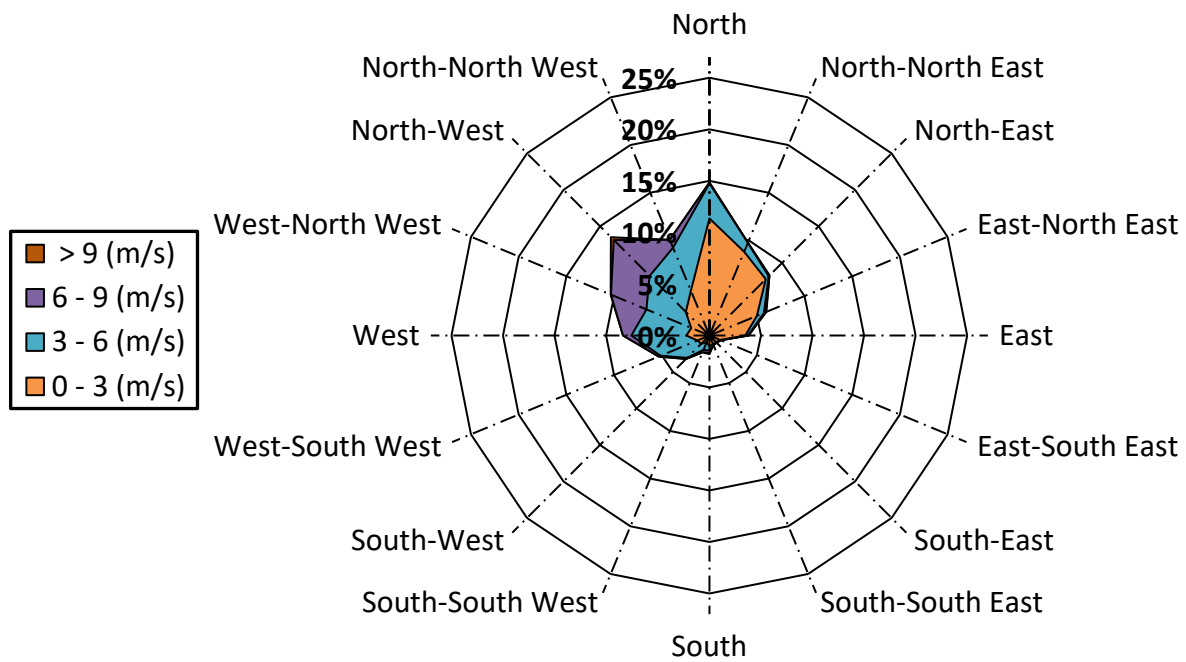


Fig. 9. Wind rose and direction for 10 m altitude

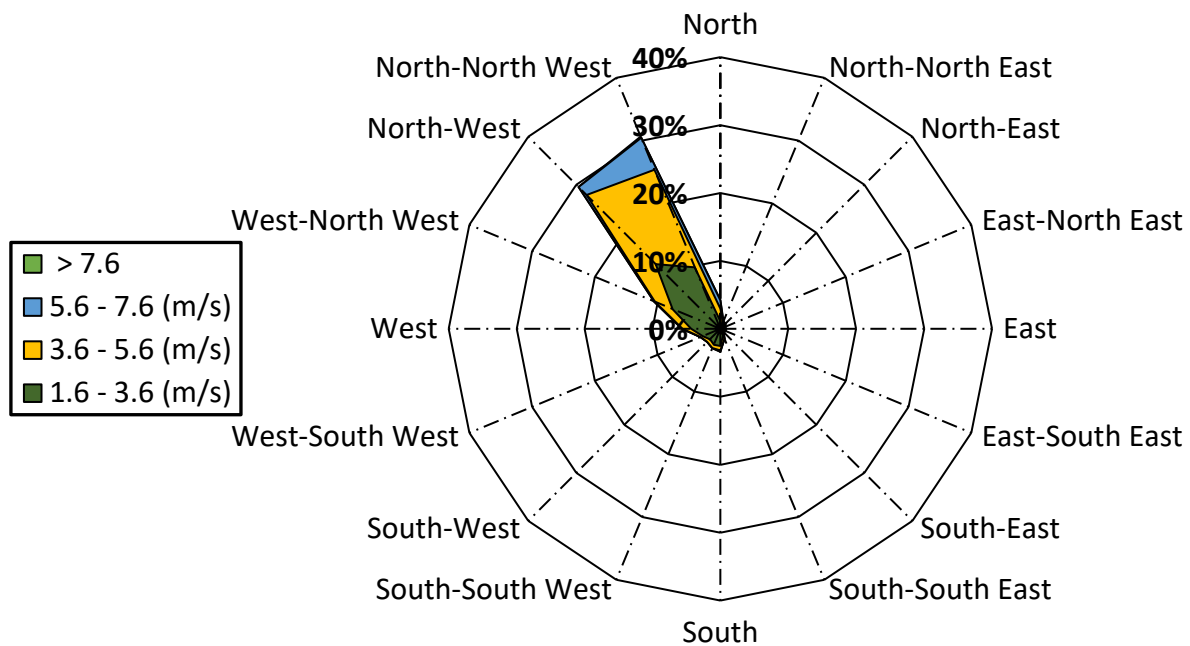


Fig. 10. The wind rose and direction for 80 m altitude

3.5 Global Solar Radiation (H_h)

The global solar radiation simply is the summation of direct and diffused radiations measured in (MJm^2). Figure 11 and Table 3 demonstrate the global solar radiation for Jeddah between (2010 and 2019). From the figure, it can be observed that June had always the highest global solar radiation

scoring 28.83 MJm² at the highest occurred in 2016. The least scoring occurred at the beginning and the end of the year achieving 15.15 MJm² in 2015 during December. Nevertheless, global solar radiation is heavily correlated with the reflected and diffused radiation which is shown clearly in Figure 12. It has been noticed that the highest global solar radiation occurred always when the highest diffused solar radiation occurred which indicates a proportional relationship. Furthermore, the diffused solar radiation is referred to the scattered radiations and beams hitting an object at different angles which are the total opposite of the direct radiation. The excursion in global solar radiation can be resulted due to the precipitation rate at the location and lower air mass.

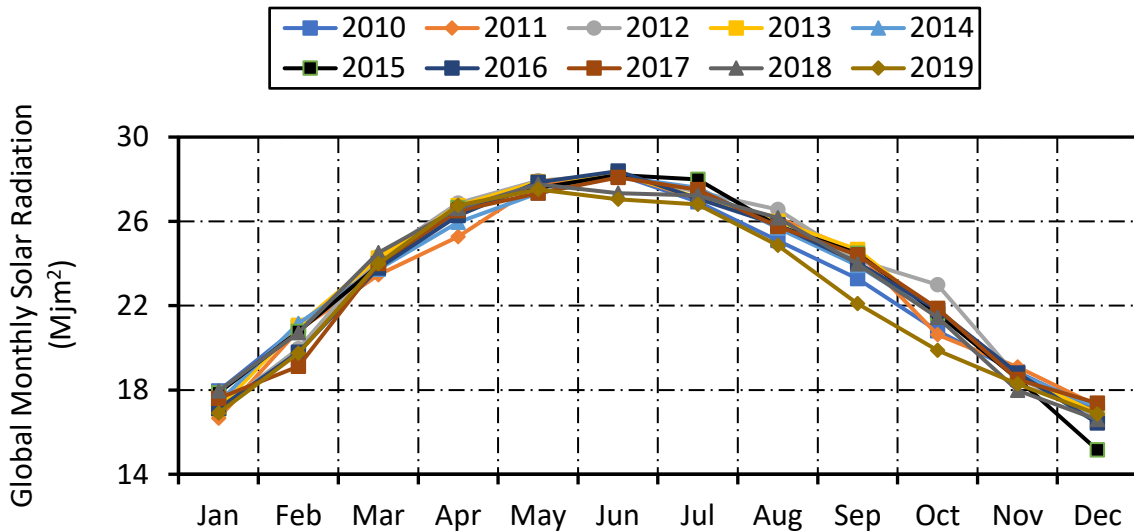


Fig. 11. Global monthly solar radiation for every year between (2010-2019)

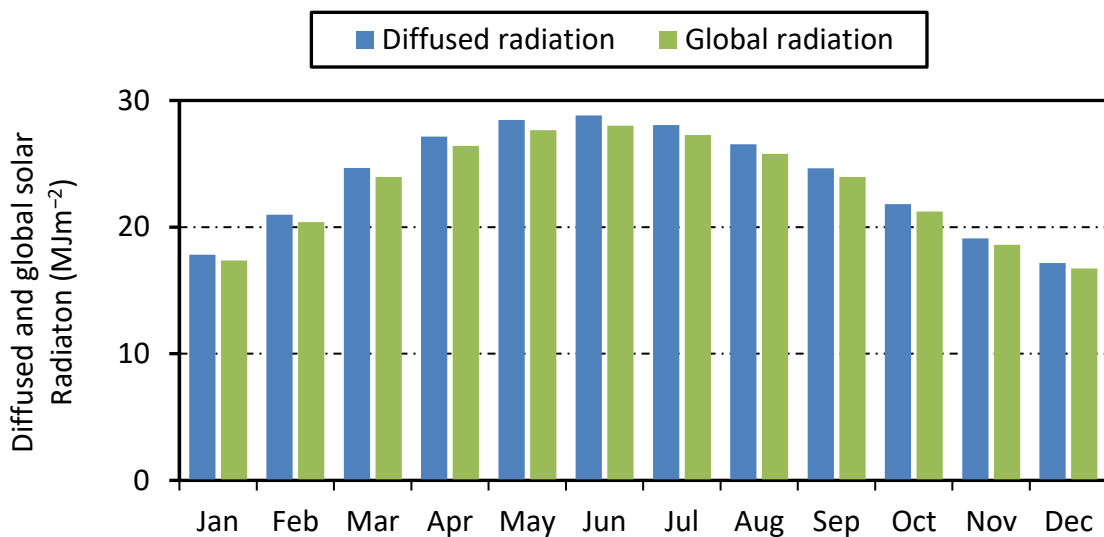


Fig. 12. Comparison between diffused and global solar radiations (MJm²) for every year between (2010-2019)

Table 3
 Global monthly solar radiation (MJm²) for every year between (2010-2019)

Year	Jan	Feb	Mar	Apr	May	Jun	Jul	Aug	Sep	Oct	Nov	Dec
2010	17.94	20.99	23.93	26.45	27.70	28.22	26.92	25.08	23.28	20.80	18.85	17.05
2011	16.66	20.83	23.46	25.27	27.74	28.27	27.07	26.18	24.54	20.62	19.08	17.25
2012	17.08	19.96	24.32	26.86	27.93	28.22	27.40	26.55	24.16	22.99	18.59	16.72
2013	17.09	21.07	24.25	26.74	27.88	28.26	27.14	26.00	24.66	21.59	18.71	16.89
2014	17.40	21.16	23.73	25.96	27.33	28.12	27.59	25.67	23.91	21.55	18.77	17.17
2015	17.86	20.78	23.90	26.65	27.57	28.20	27.98	25.78	24.48	21.63	18.53	15.15
2016	17.12	19.79	23.78	26.27	27.86	28.38	27.08	25.84	24.05	21.80	18.79	16.43
2017	17.60	19.12	24.00	26.50	27.34	28.08	27.51	25.75	24.40	21.86	18.50	17.37
2018	17.95	20.72	24.50	26.61	27.76	27.33	27.23	26.17	23.98	21.45	17.98	16.59
2019	16.90	19.73	24.00	26.75	27.51	27.04	26.80	24.87	22.09	19.88	18.28	16.86

4. Conclusion

In this study, an assessment of wind and solar energy in the city of Jeddah, Saudi Arabia has been analyzed using ten years of data from 2010 to 2019. The wind power assessment involved the use of the Weibull distribution function at 10 m and 80 m altitudes, while the Angstrom technique was used for the solar assessments. The results show that the wind speed increases with height and therefore, the 80 m altitude wind is found to be higher than 10 m altitudes, with respective highest wind speeds over the ten years being 4.36 m/s and 3.72 m/s. In terms of seasonal variation, the highest wind speed falls always during the summer solstice which starts from June to September.

Moreover, the shape and scale parameters were 1.75 and 3.56 m/s at the 10 m altitude and were respectively 5.15 and 7.80 m/s at 80 m altitudes. Meanwhile, the wind power density and wind energy density were found to be 44.09 W/m² and 285.46 kWh/m², respectively for the 10 m altitudes, while for 80 m altitude was 192.19 W/m² and 247.29 kWh/m², respectively. The highest frequency of wind speed was in the range between 4.00 to 4.99 (m/s) scoring 25.7%. The prevailing wind direction at the location chosen for 10 m and 80 m altitudes were north and north-northwest with frequencies of 11,864 and 11,572, respectively over the years 2010 to 2019.

While the solar energy potentiality on the other hand achieved the highest radiation and Angstrom's ratio during the summer in the middle of the year (May, June, and July). Furthermore, the location has an average potentiality of global solar radiation of 23.13 MJm² during the 10 years period (2010-2019), which is high as it emphasizes its utilization. Nevertheless, global solar radiation is heavily correlated with reflected and diffused radiations. It has been noticed that the highest global solar radiation occurred always when the highest diffused solar radiation occurred which indicates a proportional relationship.

Acknowledgement

The authors would like to acknowledge the financial support provided by the Universiti Tun Hussein Onn Malaysia through the H919 grant.

References

- [1] Al-Ghriybah, Mohanad, Mohd Fadhli Zulkafli, Djamel Hissein Didane, and Sofian Mohd. "Review of the recent power augmentation techniques for the Savonius wind turbines." *Journal of Advanced Research in Fluid Mechanics and Thermal Sciences* 60, no. 1 (2019): 71-84.
- [2] Freije, Afnan Mahmood, Tahani Hussain, and Eman Ali Salman. "Global warming awareness among the University of Bahrain science students." *Journal of the Association of Arab Universities for Basic and Applied Sciences* 22 (2017): 9-16. <https://doi.org/10.1016/j.jaubas.2016.02.002>
- [3] Inglesi-Lotz, Roula. "The impact of renewable energy consumption to economic growth: A panel data application."

- Energy Economics* 53 (2016): 58-63. <https://doi.org/10.1016/j.eneco.2015.01.003>
- [4] Conti-Ramsden, John, and Kirsten Dyer. "Materials innovations for more efficient wind turbines." *Renewable Energy Focus* 16, no. 5-6 (2015): 132-133. <https://doi.org/10.1016/j.ref.2015.10.013>
- [5] Kaplan, Yusuf Alper. "Overview of wind energy in the world and assessment of current wind energy policies in Turkey." *Renewable and Sustainable Energy Reviews* 43 (2015): 562-568. <https://doi.org/10.1016/j.rser.2014.11.027>
- [6] Didane, Djamel Hissein, Muhammad Amir Zafran Saipul Anuar, Mohd Faizal Mohideen Batcha, Kamil Abdullah, Mas Fawzi Mohd Ali, and Akmal Nizam Mohammed. "Simulation study on the performance of a counter-rotating savonius vertical axis wind turbine." *CFD Letters* 12, no. 4 (2020): 1-11. <https://doi.org/10.37934/cfdl.12.4.111>
- [7] Halmy, Muhammad Syahmy Mohd, Djamel Hissein Didane, Lukmon Owolabi Afolabi, and Sami Al-Alimi. "Computational Fluid Dynamics (CFD) Study on the Effect of the Number of Blades on the Performance of Double-Stage Savonius Rotor." *CFD Letters* 13, no. 4 (2021): 1-10. <https://doi.org/10.37934/cfdl.13.4.110>
- [8] Didane, Djamel Hissein, Siti Masyafikah Maksud, Mohd Fadhli Zulkafli, Nurhayati Rosly, Syariful Syafiq Shamsudin, and Amir Khalid. "Performance investigation of a small Savonius-Darrius counter-rotating vertical-axis wind turbine." *International Journal of Energy Research* 44, no. 12 (2020): 9309-9316. <https://doi.org/10.1002/er.4874>
- [9] Loutun, Mark Jason Thomas, Djamel Hissein Didane, Mohd Faizal Mohideen Batcha, Kamil Abdullah, Mas Fawzi Mohd Ali, Akmal Nizam Mohammed, and Lukmon Owolabi Afolabi. "2D CFD Simulation Study on the Performance of Various NACA Airfoils." *CFD Letters* 13, no. 4 (2021): 38-50. <https://doi.org/10.37934/cfdl.13.4.3850>
- [10] Caglayan, Dilara Gulcin, David Severin Ryberg, Heidi Heinrichs, Jochen Linßen, Detlef Stolten, and Martin Robinius. "The techno-economic potential of offshore wind energy with optimized future turbine designs in Europe." *Applied Energy* 255 (2019): 113794. <https://doi.org/10.1016/j.apenergy.2019.113794>
- [11] Adam, Aminu Dankaka, and Gokhan Apaydin. "Grid connected solar photovoltaic system as a tool for green house gas emission reduction in Turkey." *Renewable and Sustainable Energy Reviews* 53 (2016): 1086-1091. <https://doi.org/10.1016/j.rser.2015.09.023>
- [12] Ulloa-Godinez, H. Héctor, E. Mario García-Guadalupe, U. Hermes Ramírez-Sánchez, C. Jorge Regla-Carrillo, and L. Aida Fajardo-Montiel. "Solar radiation data for the state of Jalisco and Guadalajara metropolitan zone, Mexico." *Computational Water, Energy, and Environmental Engineering* 6, no. 03 (2017): 205-228. <https://doi.org/10.4236/cweee.2017.63015>
- [13] Maradin, Dario, Ljerka Cerović, and Trina Mjeda. "Economic effects of renewable energy technologies." *Naše gospodarstvo/Our Economy* 63, no. 2 (2017): 49-59. <https://doi.org/10.1515/ngoe-2017-0012>
- [14] Alshehry, Atef Saad, and Mounir Belloumi. "Energy consumption, carbon dioxide emissions and economic growth: The case of Saudi Arabia." *Renewable and Sustainable Energy Reviews* 41 (2015): 237-247. <https://doi.org/10.1016/j.rser.2014.08.004>
- [15] Tlili, Iskander. "Renewable energy in Saudi Arabia: current status and future potentials." *Environment, Development and Sustainability* 17, no. 4 (2015): 859-886. <https://doi.org/10.1007/s10668-014-9579-9>
- [16] Baradie, Khalid I. *The Development of Power Systems in Saudi Arabia*. Technical Report. Dhahran, Saudi Arabia: King Fahd University of Petroleum and Minerals Department of Electrical Engineering, 2015.
- [17] Bilir, Levent, Mehmet Imir, Yilser Devrim, and Ayhan Albostan. "Seasonal and yearly wind speed distribution and wind power density analysis based on Weibull distribution function." *International Journal of Hydrogen Energy* 40, no. 44 (2015): 15301-15310. <https://doi.org/10.1016/j.ijhydene.2015.04.140>
- [18] Al-Ghriybah, Mohanad, Mohd Fadhli Zulkafli, Djamel Hissein Didane, and Sofian Mohd. "Wind energy assessment for the capital city of Jordan, Amman." *Journal of Applied Engineering Science* 17, no. 3 (2019): 311-320. <https://doi.org/10.5937/jaes17-20241>
- [19] Saeed, M. Khalid, Abdul Salam, Anees Ur Rehman, and M. Abid Saeed. "Comparison of six different methods of Weibull distribution for wind power assessment: A case study for a site in the Northern region of Pakistan." *Sustainable Energy Technologies and Assessments* 36 (2019): 100541. <https://doi.org/10.1016/j.seta.2019.100541>
- [20] Yıldırım, H. Başak, Özgür Çelik, Ahmet Teke, and Burak Barutçu. "Estimating daily Global solar radiation with graphical user interface in Eastern Mediterranean region of Turkey." *Renewable and Sustainable Energy Reviews* 82 (2018): 1528-1537. <https://doi.org/10.1016/j.rser.2017.06.030>
- [21] Didane, Djamel Hissein, Nurhayati Rosly, Mohd Fadhli Zulkafli, and Syariful Syafiq Shamsudin. "Evaluation of wind energy potential as a power generation source in Chad." *International Journal of Rotating Machinery* 2017 (2017). <https://doi.org/10.1155/2017/3121875>
- [22] Didane, Djamel Hissein, Abas Ab Wahab, Syariful Syafiq Shamsudin, Nurhayati Rosly, Mohd Fadhli Zulkafli, and Sofian Mohd. "Assessment of wind energy potential in the capital city of Chad, N'Djamena." In *AIP Conference Proceedings*, vol. 1831, no. 1, p. 020049. AIP Publishing LLC, 2017. <https://doi.org/10.1063/1.4981190>
- [23] Hassane, Abdelhamid Issa, Djamel Hissein Didane, Abakar Mahamat Tahir, and Jean-Marie Hauglustaine. "Wind and Solar Assessment in the Sahelian Zone of Chad." *International Journal of Integrated Engineering* 10, no. 8

- (2018): 164-174. <https://doi.org/10.30880/ijie.2018.10.08.026>
- [24] Ramli, Makbul A. M., Ayong Hiendro, and Yusuf A. Al-Turki. "Techno-economic energy analysis of wind/solar hybrid system: Case study for western coastal area of Saudi Arabia." *Renewable Energy* 91 (2016): 374-385. <https://doi.org/10.1016/j.renene.2016.01.071>
- [25] Zell, Erica, Sami Gasim, Stephen Wilcox, Suzan Katamoura, Thomas Stoffel, Husain Shibli, Jill Engel-Cox, and Madi Al Subie. "Assessment of solar radiation resources in Saudi Arabia." *Solar Energy* 119 (2015): 422-438. <https://doi.org/10.1016/j.solener.2015.06.031>
- [26] Rehman, Shafiqur, and Aftab Ahmad. "Assessment of wind energy potential for coastal locations of the Kingdom of Saudi Arabia." *Energy* 29, no. 8 (2004): 1105-1115. <https://doi.org/10.1016/j.energy.2004.02.026>